Bi-directional mapping between polarization and spatially encoded photonic qutrits

Qing Lin[1,*] and Bing He[2,†]
[1]*College of Information Science and Engineering, Huaqiao University–Xiamen, Xiamen 361021, China*
[2]*Institute for Quantum Information Science, University of Calgary, Alberta, Canada T2N 1N4*
(Received 9 June 2009; revised manuscript received 13 August 2009; published 7 December 2009)

Qutrits, the triple level quantum systems in various forms, have been proposed for quantum information processing recently. By the methods presented in this paper, a biphotonic qutrit, which is encoded with the polarizations of two photons in the same spatial-temporal mode, can be mapped to a single-photon qutrit in spatial modes. It will make arbitrary unitary operation on such biphotonic qutrit possible if we can also realize the inverse map to polarization space. Among the two schemes proposed in this paper, the one based only on linear optics realizes an arbitrary U(3) operation with a very small success probability. However, if added with weak nonlinearity, the success probability can be greatly improved. These schemes are feasible with the current experimental technology.

DOI: 10.1103/PhysRevA.80.062312 PACS number(s): 03.67.Lx, 42.50.Ex

I. INTRODUCTION

Quantum communications and quantum computation apply quantum states to store and transmit information. The capacity of a state for the purpose is dependent on its dimension, so the higher dimension of a state means the higher capacity to carry information. In addition, the use of higher-dimensional quantum states, e.g., qudits and entangled qudits, enjoys many advantages such as enhanced security in quantum cryptography [1], more efficient quantum logic gate [2], and others. Qudits and entangled qudits therefore attract many researches recently. The proposals for generating qudits and entangled qudits include orbital angular-momentum-entangled qutrits [3], pixel-entangled qudits [4], energy-time-entangled and time-bin-entangled qudits [5], and biphotonic qutrits encoded with polarization degree of freedom [6–8]. In this paper, we will focus on biphotonic qutrits which are represented with the polarizations of two photons in the same spatial-temporal mode [9]—$|0\rangle_3 \equiv |HH\rangle$, $|1\rangle_3 \equiv |HV\rangle$, and $|2\rangle_3 \equiv |VV\rangle$, where H and V denote the horizontal and vertical polarizations, respectively. The generation of such qutrits including the entangled ones has been demonstrated [6,8]. In an recent work by Lanyon *et al.* [8], with an ancilla qubit and a Fock state filter associated with some wave plates, a biphotonic state as the linear combination of $\{|0\rangle_3, |1\rangle_3, |2\rangle_3\}$ is generated from the logic state $|0\rangle_3$. To manipulate a biphotonic qutrit in this form, one should know how to implement a unitary operation on such qutrits. However, due to the indistinguishableness of two photons in the same spatial-temporal mode, it is very difficult to realize a simple unitary operation on such biphotonic qutrit [10]. Here we present two schemes realizing the transformation from a biphotonic qutrit to any other biphotonic qutrit, i.e., arbitrary unitary operations U(3) on biphotonic qutrits. The schemes work with transforming the input biphotonic qutrits to the corresponding single-photon qutrits in spatial modes and then mapping the single-photon qutrits back to the original polarization modes of two photons.

The rest of the paper is organized as follows. In Sec. II, we present a purely linear optical scheme of the transformation and inverse transformation from a biphotonic qutrit in the same spatial-temporal mode to the corresponding single-photon qutrit. In Sec. III, we improve on the linear optical scheme with weak cross-Kerr nonlinearity, making the realization of bi-directional mapping much more efficient. Section IV concludes the work with a brief discussion.

II. BI-DIRECTIONAL MAPPING WITH LINEAR OPTICAL ELEMENTS

Any unitary operation on a single-photon qudits in spatial modes can be performed by a linear optical multiport interferometer (LOMI) [11]. It is therefore possible to manipulate biphotonic qutrits following such strategy: first, transform a biphotonic qutrit to a single-photon qutrit, then perform the desired operations on this single-photon qutrit, and finally transform the single-photon qutrit back to a biphotonic qutrit. In what follows, we present the details of the procedure, which is realized only with linear optical elements.

A. Transforming biphoton qutrit to single-photon qutrit

Suppose a biphotonic qutrit is initially prepared as

$$|\psi\rangle_{in} = \alpha|0\rangle_3 + \beta|1\rangle_3 + \gamma|2\rangle_3, \tag{1}$$

where $|\alpha|^2+|\beta|^2+|\gamma|^2=1$. The operations shown in Fig. 1 implement the map

$$|\psi\rangle_{in} \to \alpha|0\rangle_S + \beta|1\rangle_S + \gamma|2\rangle_S = |\psi\rangle_S, \tag{2}$$

where $|\psi\rangle_S$ is a single-photon qutrit encoded with the spatial modes $|i\rangle_S$ $(i=0,1,2)$ of the single photon. Here we first apply a variable beam splitter (VBS) to the input biphotonic qutrit, realizing the following transformation:

*qlin@mail.ustc.edu.cn
†bhe98@earthlink.net

 ©2009 The American Physical Society

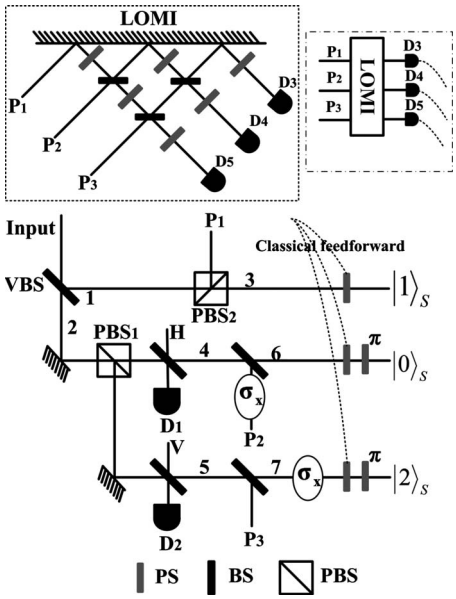

FIG. 1. Schematic setup for the transformation from a biphotonic qutrit to the corresponding single-photon qutrit. At first, the input qutrit is transmitted through a VBS and then the two output modes are transmitted through a PBS, respectively. Two single photons are used as the ancillas, which will interfere with the output modes of PBS_1. The part in dashed line is used to erase the path information of the modes P_1,P_2,P_3, which are all in the state $|V\rangle$. The detection results are used as control signals of the conditional phase shift summarized in Table I through the classical feed forward. By the proper post selection, the biphotonic qutrit can be transformed to the corresponding single-photon qutrit as in Eq. (2). For details, see the text.

$$\left(\frac{\alpha}{\sqrt{2}}a_H^{\dagger 2}+\beta a_H^\dagger a_V^\dagger+\frac{\gamma}{\sqrt{2}}a_V^{\dagger 2}\right)|\text{vac}\rangle \rightarrow \left[\frac{\alpha}{\sqrt{2}}(ra_{H1}^\dagger+ta_{H2}^\dagger)^2+\beta(ra_{H1}^\dagger+ta_{H2}^\dagger)(ra_{V1}^\dagger+ta_{V2}^\dagger)+\frac{\gamma}{\sqrt{2}}(ra_{V1}^\dagger+ta_{V2}^\dagger)^2\right]|\text{vac}\rangle, \tag{3}$$

where 1 and 2 denote the different paths and t (r) is the transmissivity (reflectivity) of the VBS.

Next, in order to project out the proper components, we introduce two single photons $|H\rangle$ and $|V\rangle$ as the ancilla and make them interfere with the output modes of the polarizing beam splitters (PBS_1) on two 50:50 beam splitters (BS), respectively. Due to the Hong-Ou-Mandal interference effect [12], two indistinguishable photons will be bunching to the same output mode of BS and then we can use the proper post selection to get the desired components. To see the details, we show the evolution of each input mode of two photons as follows:

$$a_{H1}^\dagger \rightarrow a_{H3}^\dagger, a_{H2}^\dagger \rightarrow \frac{1}{\sqrt{2}}(a_{H4}^\dagger+a_{HD_1}^\dagger),$$

$$a_{V1}^\dagger \rightarrow a_{VP_1}^\dagger, a_{V2}^\dagger \rightarrow \frac{1}{\sqrt{2}}(a_{V5}^\dagger+a_{VD_2}^\dagger), \tag{4}$$

where the subscripts D_1,D_2 denote the modes going to photon number nonresolving detectors. Meanwhile, for the ancilla photons, the evolutions are

$$a_H^\dagger \rightarrow \frac{1}{\sqrt{2}}(a_{H4}^\dagger-a_{HD_1}^\dagger),$$

$$a_V^\dagger \rightarrow \frac{1}{\sqrt{2}}(a_{V5}^\dagger-a_{VD_2}^\dagger). \tag{5}$$

The 50:50 BS placed on path 4 (5) is to split the mode 4 (5) into two output modes $6,P_2$ ($7,P_3$), making the transformations

$$a_{H4}^\dagger \rightarrow \frac{1}{\sqrt{2}}(a_{H6}^\dagger+a_{HP_2}^\dagger) \rightarrow \frac{1}{\sqrt{2}}(a_{H6}^\dagger+a_{VP_2}^\dagger),$$

$$a_{V5}^\dagger \rightarrow \frac{1}{\sqrt{2}}(a_{V7}^\dagger+a_{VP_3}^\dagger) \rightarrow \frac{1}{\sqrt{2}}(a_{H7}^\dagger+a_{VP_3}^\dagger). \tag{6}$$

After that, one obtains the following state:

$$\left(-\frac{\alpha}{4\sqrt{2}}t^2a_{H6}^\dagger a_{VP_2}^\dagger+\frac{\beta}{2}r^2a_{H3}^\dagger a_{VP_1}^\dagger-\frac{\gamma}{4\sqrt{2}}t^2a_{V7}^\dagger a_{VP_3}^\dagger\right)a_{HD_1}^\dagger a_{VD_2}^\dagger|\text{vac}\rangle+\mathcal{C}, \tag{7}$$

where $\mathcal{C}$ denotes the components of two photons appearing in the same spatial mode. If we discard the modes P_1,P_2,P_3 without changing anything else, i.e., erase the path information of P_1,P_2,P_3, the first three terms in Eq. (7) will be just the desired single-photon qutrit, which carries the same coefficients of the input biphoton qutrit. Since there is only one photon in the modes P_1,P_2,P_3, we will use a quantum Fourier transform (QFT) (j,k' denote the spatial modes) [13],

$$a_{Vj}^\dagger|\text{vac}\rangle=\frac{1}{\sqrt{3}}\sum_{k'=0}^{2}e^{2\pi ijk/3}a_{Vk'}^\dagger|\text{vac}\rangle, \tag{8}$$

to do it. The QFT is an unitary operation for a single photon in three spatial modes, so we can use an LOMI shown in the dashed line of Fig. 1 to implement it. Just like the setups in the dash-dotted line, three photon number nonresolving detectors are used and the detection results are to control the conditional phase shift (PS) through classical feed forward. The relations between the detection results and the corresponding PS operations are summarized in Table I. After that, with the coincident measurements of the detectors D_1,D_2, and one of the detectors D_3,D_4,D_5, the state

$$\left(\frac{\alpha}{4\sqrt{2}}t^2a_{H6}^\dagger+\frac{\beta}{2}r^2a_{H3}^\dagger+\frac{\gamma}{4\sqrt{2}}t^2a_{V7}^\dagger\right)|\text{vac}\rangle \tag{9}$$

will be projected out by the post selection. We can rewrite it as

TABLE I. The relations between the detections and the corresponding phase shifters on paths 3, 6, and 7.

	D_3	D_4	D_5
3	0	0	0
6	0	$\frac{2\pi}{3}$	$\frac{4\pi}{3}$
7	0	$\frac{4\pi}{3}$	$\frac{8\pi}{3}$

$$\frac{\alpha}{4\sqrt{2}}t^2|H\rangle_6 + \frac{\beta}{2}r^2|H\rangle_3 + \frac{\gamma}{4\sqrt{2}}t^2|V\rangle_7. \tag{10}$$

It is straightforward that the state will be $|\psi\rangle_S$, given that $t^2 = 2\sqrt{2}r^2$ or $t^2 = \frac{2\sqrt{2}}{1+2\sqrt{2}}$. The corresponding success probability of the process is $(\frac{t^2}{4\sqrt{2}})^2 = 1.71\times 10^{-2}$.

B. Transformation back to biphotonic qutrit

After the desired operations performed on the single-photon qutirt, we should transform the single-photon qutrit $|\psi'\rangle_S = \alpha'|0'\rangle_S + \beta'|1'\rangle_S + \gamma'|2'\rangle_S$ back to a biphotonic qutrit. The inverse transformation is shown in Fig. 2. Three VBSs ($\mathrm{VBS}_1, \mathrm{VBS}_2, \mathrm{VBS}_3$) with the transmissivities (reflectivities) t_1, t_2, t_3 (r_1, r_2, r_3), two PSs, and σ_x operations are applied to perform the transformation

$$(\alpha' a^\dagger_{H0'} + \beta' a^\dagger_{H1'} + \gamma' a^\dagger_{H2'})|\mathrm{vac}\rangle \to [(\alpha' r_2 - \beta' t_1 t_2)a^\dagger_{H1} + \beta' r_1 a^\dagger_{H2} + \gamma' t_3 a^\dagger_{V3}]|\mathrm{vac}\rangle. \tag{11}$$

In order to select out the desired components, we introduce a single photon $|H\rangle$ as an ancilla, which will interfere with the mode 1 through a 50:50 BS and meanwhile combine the modes 2 and 3 by a PBS into the mode 5, which will then interfere with another ancilla single photon $|V\rangle$ through a 50:50 BS. The total state will be then transformed to

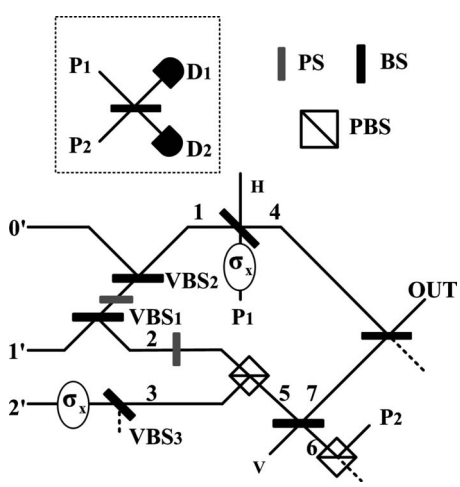

FIG. 2. Schematic setup for the inverse transformation from a single-photon qutrit back to a biphoton qutrit. Two VBSs are applied and two extra single photons work as the ancilla. The single-photon qutrit can be transformed back to a biphotonic qutrit by post selection. For details, see the text.

$$\left\{\frac{1}{2\sqrt{2}}(\alpha' r_2 - \beta' t_1 t_2)(a^{\dagger 2}_{H4} - a^{\dagger 2}_{HP_1})(a^\dagger_{V7} - a^\dagger_{V6}) + \frac{1}{2\sqrt{2}}\beta' r_1 (a^\dagger_{H4} - a^\dagger_{HP_1})(a^\dagger_{H7} + a^\dagger_{H6})(a^\dagger_{V7} - a^\dagger_{V6}) + \frac{1}{2\sqrt{2}}\gamma' t_3 (a^\dagger_{H4} - a^\dagger_{HP_1})(a^{\dagger 2}_{V7} - a^{\dagger 2}_{V6})\right\}|\mathrm{vac}\rangle. \tag{12}$$

The $|V\rangle$ mode on path 6 will be reflected to mode P_2. Now, the following state can be achieved:

$$-\frac{1}{2\sqrt{2}}[(\alpha' r_2 - \beta' t_1 t_2)a^{\dagger 2}_{H4} a^\dagger_{VP_2} + \beta' r_1 (a^\dagger_{H7} a^\dagger_{V7} a^\dagger_{HP_1} + a^\dagger_{H4} a^\dagger_{H7} a^\dagger_{VP_2}) + \gamma' t_3 a^{\dagger 2}_{V7} a^\dagger_{HP_1}]|\mathrm{vac}\rangle + \mathcal{C}. \tag{13}$$

The left work will be the erasure of the path information of the modes P_1, P_2 by the detection similar to that in Sec. II A. Because there are only two spatial modes, the realization of the QFT will be simplified with just one 50:50 BS as shown in dashed line. Now, the state

$$-\frac{1}{4}[(\alpha' r_2 - \beta' t_1 t_2)a^{\dagger 2}_{H4} + \beta' r_1 (a^\dagger_{H7} a^\dagger_{V7} + a^\dagger_{H4} a^\dagger_{H7}) + \gamma' t_3 a^{\dagger 2}_{V7}]a^\dagger_{VD_1}|\mathrm{vac}\rangle + \mathcal{C} \tag{14}$$

can be achieved, where we only keep the terms with the photonic modes on P_1, P_2 being detected by the detector D_1. In the other case, when the photon is detected by the detector D_2, there will be an additional phase shift π to the components including $a^\dagger_{VP_2}$ and it seems difficult to remove it by a simple operation.

After the erasure of P_1 and P_2 modes, the modes 4 and 7 will interfere with each other through a 50:50 BS. If there are two photons in the final output (which can be realized by common biphotonic qutrit tomograph [8]) and a click on one of the two detectors D_1, D_2, we will project out the state

$$-\frac{1}{8}[(\alpha' r_2 - \beta' t_1 t_2)a^{\dagger 2}_{H\ out} + \beta' r_1 (a^\dagger_{H\ out} a^\dagger_{V\ out} + a^{\dagger 2}_{H\ out}) + \gamma' t_3 a^{\dagger 2}_{V\ out}]|\mathrm{vac}\rangle = -\frac{1}{8}[(\alpha' r_2 - \beta' t_1 t_2 + \beta' r_1)a^{\dagger 2}_{H\ out} + \beta' r_1 a^\dagger_{H\ out} a^\dagger_{V\ out} + \gamma' t_3 a^{\dagger 2}_{V\ out}]|\mathrm{vac}\rangle \tag{15}$$

by post selection. Choosing $t_1 t_2 = r_1$ and $\sqrt{2}r_2 = r_1$, i.e., $t_1^2 = \frac{\sqrt{17}-3}{2}(r_1^2 = \frac{5-\sqrt{17}}{2})$, associated with $t_3^2 = \frac{5-\sqrt{17}}{4}$, we can achieve the final state

$$\frac{r_1}{8}\left(\frac{\alpha'}{\sqrt{2}}a^{\dagger 2}_{H\ out} + \beta' a^\dagger_{H\ out} a^\dagger_{V\ out} + \frac{\gamma'}{\sqrt{2}}a^{\dagger 2}_{V\ out}\right)|\mathrm{vac}\rangle, \tag{16}$$

which is the target biphotonic qutrit $\alpha'|0\rangle_3 + \beta'|1\rangle_3 + \gamma'|2\rangle_3$. The corresponding success probability is $(\frac{r_1}{8})^2 = 6.85\times 10^{-3}$. Associated with the above transformation, we could manipu-

late the biphotonic qutrits, such as perform an arbitrary unitary operation U(3) on them, with a success probability $1.71\times 6.85\times 10^{-5}=1.17\times 10^{-4}$. The scheme succeeds with a very small probability, but in principle, it can realize any unitary operation on a biphoton qutrit.

In summary, with four ancilla single photons, we could realize arbitrary manipulation with linear optical elements and coincidence measurements. Since only two cases—no photon or any number of photons—should be discriminated, the common photon number nonresolving detector, e.g., silicon avalanche photodiodes (APDs) will be necessary for the scheme.

III. BI-DIRECTIONAL MAPPING WITH WEAK CROSS-KERR NONLINEARITY

The success probability of the above scheme with only linear optical elements could be too small for practical application. This success probability, however, can be greatly increased if we apply some weak nonlinearity in the circuit. The application of weak cross-Kerr nonlinearity has been proposed in various fields of quantum information science. It was first applied to realize parity projector [14] and deterministic CNOT gate [15] and then in some quantum computation and communication schemes (see, e.g., [16–18]). The effective Hamiltonian for cross-Kerr nonlinearity is $\mathcal{H}=-\hbar\chi\hat{n}_i\hat{n}_j$ (χ is the nonlinear intensity and $\hat{n}_{i/j}$ the number operator of the interacting modes). The cross-phase-modulation (XPM) process caused by such interaction between a Fock state $|n\rangle$ and a coherent state $|\alpha\rangle$ gives rise to the transformation, $|n\rangle|\alpha\rangle\rightarrow|n\rangle|\alpha e^{i\theta}\rangle$, where $\theta=\chi t$ induced during the interaction time t could be small with weak nonlinearity. Another useful technique to our scheme is homodyne-heterodyne measurement for the quadratures of coherent state. A statelike $\Sigma_k|k\rangle|\alpha e^{ik\theta}\rangle$ can be projected to a definite Fock state or a superposition of some Fock states by such measurement, which can be performed with high fidelity.

A. Transformation with XPM process

With weak cross-Kerr nonlinearity, we implement the transformation from a biphotonic qutrit to a single-photon qutrit as shown in Fig. 3. An initial biphotonic qutrit in the state $|\psi\rangle_{in}$ of Eq. (1) is first sent to a 50:50 BS, making the following transformation:

$$\left(\frac{\alpha}{\sqrt{2}}a_H^{\dagger 2}+\beta a_H^\dagger a_V^\dagger+\frac{\gamma}{\sqrt{2}}a_V^{\dagger 2}\right)|\text{vac}\rangle\rightarrow\left[\frac{\alpha}{2\sqrt{2}}(a_{H1}^\dagger+a_{H2}^\dagger)^2+\frac{\beta}{2}(a_{H1}^\dagger+a_{H2}^\dagger)(a_{V1}^\dagger+a_{V2}^\dagger)+\frac{\gamma}{2\sqrt{2}}(a_{V1}^\dagger+a_{V2}^\dagger)^2\right]|\text{vac}\rangle. \tag{17}$$

Next a VBS is placed on path 2 such that

$$a_{H2}^\dagger\rightarrow ra_{H3}^\dagger+ta_{H4}^\dagger,$$
$$a_{V2}^\dagger\rightarrow ra_{V3}^\dagger+ta_{V4}^\dagger. \tag{18}$$

Then, after three PBSs change the spatial modes as $1\rightarrow 1,1'$, $3\rightarrow 5,6$, and $4\rightarrow 7$, two qubus beams (i.e., coherent states) $|\alpha_1\rangle|\alpha_2\rangle$ will be coupled to the corresponding photonic modes through the XPM processes in two quantum nondemolition detection (QND) modules, which are shown in dashed line of Fig. 3. The result will be the following transformation of the total system:

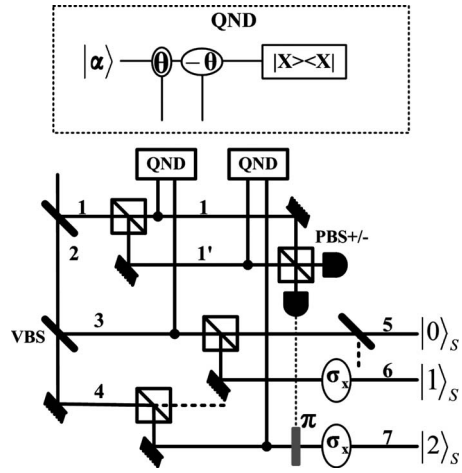

FIG. 3. Schematic setup for the transformation with XPM process. Two QND modules working with XPM process are used here. The transformation is realized under the condition that the two qubus beams pick no phase shift, with the corresponding success probability 1/6. For the details, see text.

$$\left(\frac{\alpha}{\sqrt{2}}ra_{H1}^\dagger a_{H5}^\dagger+\frac{\beta}{2}ra_{H1}^\dagger a_{V6}^\dagger+\frac{\gamma}{\sqrt{2}}ta_{V1}^\dagger,a_{V7}^\dagger\right)|\text{vac}\rangle|\alpha_1\rangle|\alpha_2\rangle+\mathcal{C}, \tag{19}$$

where we only give the terms that two qubus beams pick no phase shift. These terms can be separated from the others by the quadrature measurement $|X\rangle\langle X|$, which is implementable with homodyne-heterodyne measurement [15,16], to obtain the following state:

$$\left(\frac{\alpha}{\sqrt{2}}ra_{H1}^\dagger a_{H5}^\dagger+\frac{\beta}{2}ra_{H1}^\dagger a_{V6}^\dagger+\frac{\gamma}{\sqrt{2}}ta_{V1}^\dagger,a_{V7}^\dagger\right)|\text{vac}\rangle=\frac{\alpha}{\sqrt{2}}r|H\rangle_1|H\rangle_5+\frac{\beta}{2}r|H\rangle_1|V\rangle_6+\frac{\gamma}{\sqrt{2}}t|V\rangle_1|V\rangle_7. \tag{20}$$

This state can be expressed as

$$\frac{\alpha}{2}r(|+\rangle_1+|-\rangle_1)|H\rangle_5+\frac{\beta}{2\sqrt{2}}r(|+\rangle_1+|-\rangle_1)|V\rangle_6+\frac{\gamma}{2}t(|+\rangle_1-|-\rangle_1)|V\rangle_7, \tag{21}$$

where $|\pm\rangle=\frac{1}{\sqrt{2}}(|H\rangle+|V\rangle)$. Now, we use a PBS$_\pm$ which transmits $|+\rangle$ and reflects $|-\rangle$ and the following two photon number nonresolving detectors. If the detection is $|+\rangle$, the state

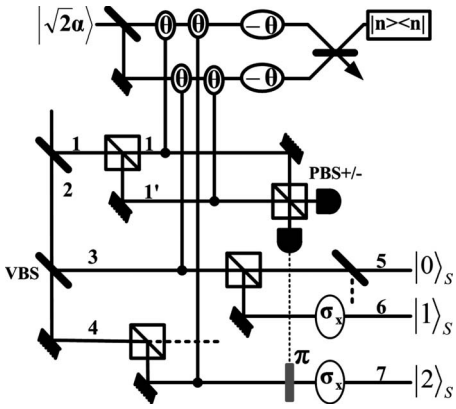

FIG. 4. Schematic setup for the transformation from biphoton qutrits to the corresponding single-photon qutrits with double XPM method. The only difference from Fig. 3 is that the two separate XPM processes are replaced by a double XPM process of two identical qubus beams. In the design, no XPM phase shift of $-\theta$ will be necessary and it makes the scheme more feasible.

$$\frac{\alpha}{\sqrt{2}}r|H\rangle_5 + \frac{\beta}{2}r|V\rangle_6 + \frac{\gamma}{\sqrt{2}}t|V\rangle_7 \tag{22}$$

will be projected out; on the other hand, if the detection is $|-\rangle$, what is realized is

$$\frac{\alpha}{\sqrt{2}}r|H\rangle_5 + \frac{\beta}{2}r|V\rangle_6 - \frac{\gamma}{\sqrt{2}}t|V\rangle_7, \tag{23}$$

which can be transform to the state in Eq. (22) by the conditional phase shifter π on path 7. By selecting $\frac{r}{2}=\frac{t}{\sqrt{2}}$, i.e., $t=\frac{1}{\sqrt{3}}$, and using a 50:50 BS for the mode 5 and two σ_x operations for modes 6, 7, we can achieve the following state:

$$\frac{1}{\sqrt{6}}(\alpha|H\rangle_5 + \beta|H\rangle_6 + \gamma|H\rangle_7), \tag{24}$$

which is the single-photon qutrit $|\psi\rangle_S$ in Eq. (2). The success probability is $\frac{1}{6}$, which is much higher than that of the linear optical scheme. Moreover, no ancilla single photon is necessary here.

The scheme is based on quadrature projection after XPM process, so it does not require any post selection by coincidence measurement. But it needs an XPM phase shift of $-\theta$, which is only possible with the equivalent phase shift $2\pi-\theta$ and could be impractical [19]. The XPM phase shift $\theta \sim 10^{-2}$ is possible with, for example, electromagnetically induced transparencies (EITs) [20], whispering-gallery microresonators [21], optical fibers [22], or cavity QED systems [23], but the corresponding $2\pi-\theta$ will be too large to realize by the available techniques. To avoid the XPM phase shift of $-\theta$, we propose a different design of the transformation shown in Fig. 4. Here we use the double XPM method in [18] to replace the two XPM processes without changing anything else.

We describe it briefly as the process is similar. In the double XPM process, two qubus beams $|\alpha\rangle|\alpha\rangle$ will be coupled to the corresponding photonic modes as shown in Fig. 4. The XPM pattern in Fig. 4 is that the first beam being coupled to the $|H\rangle$ mode on path 1 and the $|V\rangle$ mode on path 4, while the second beam to $|V\rangle$ mode on path 1′ and the modes on path 3. Suppose the XPM phase shifts induced by the couplings are all θ. After that, the total system will be transformed to

$$\begin{aligned}&\left(\frac{\alpha}{\sqrt{2}}ra_{H1}^{\dagger}a_{H3}^{\dagger} + \frac{\beta}{2}a_{H1}^{\dagger}a_{V1'}^{\dagger} + \frac{\beta}{2}ra_{H1}^{\dagger}a_{V3}^{\dagger} + \frac{\beta}{2}rta_{H3}^{\dagger}a_{V4}^{\dagger}\right.\\&\left.+\frac{\gamma}{2\sqrt{2}}ta_{V1}^{\dagger}a_{V4}^{\dagger} + \frac{\gamma}{2\sqrt{2}}rta_{V3}^{\dagger}a_{V4}^{\dagger}\right)|\text{vac}\rangle|\alpha e^{i\theta}\rangle|\alpha e^{i\theta}\rangle\\&+\frac{\alpha}{2\sqrt{2}}t^2a_{H4}^{\dagger 2}|\text{vac}\rangle|\alpha\rangle|\alpha\rangle + \mathcal{C},\end{aligned} \tag{25}$$

where $\mathcal{C}$ denotes the terms that the two qubus beams pick up the different phase shifts. A phase shifter of $-\theta$ is, respectively, applied to two qubus beams and then one more 50:50 BS implements the transformation $|\alpha_1\rangle|\alpha_2\rangle \to |\frac{\alpha_1-\alpha_2}{\sqrt{2}}\rangle|\frac{\alpha_1+\alpha_2}{\sqrt{2}}\rangle$ of the coherent-state components. The above state will be therefore transformed to

$$\begin{aligned}&\left(\frac{\alpha}{\sqrt{2}}ra_{H1}^{\dagger}a_{H3}^{\dagger} + \frac{\beta}{2}a_{H1}^{\dagger}a_{V1'}^{\dagger} + \frac{\beta}{2}ra_{H1}^{\dagger}a_{V3}^{\dagger}\right.\\&\left.+\frac{\beta}{2}rta_{H3}^{\dagger}a_{V4}^{\dagger} + \frac{\gamma}{2\sqrt{2}}ta_{V1}^{\dagger}a_{V4}^{\dagger} + \frac{\gamma}{2\sqrt{2}}rta_{V3}^{\dagger}a_{V4}^{\dagger}\right)|\text{vac}\rangle|0\rangle|\sqrt{2}\alpha\rangle\\&+\frac{\alpha}{2\sqrt{2}}t^2a_{H4}^{\dagger 2}|\text{vac}\rangle|0\rangle|\sqrt{2}\alpha\rangle + \mathcal{C}.\end{aligned} \tag{26}$$

Then, we could use the projections $|n\rangle\langle n|$ on the first qubus beam to get the proper output. If $n=0$ and by the post selection that one photon will appear on the output (5, 6, 7) while a click on one of the two detectors after the PBS$_\pm$, the state in Eq. (20) can be therefore projected out. Similar to the process in Fig. 3, we can achieve the final single-photon qutrit $|\psi\rangle_S$ with the success probability $\frac{1}{6}$. Though this design requires the post selection, it dispenses with the XPM phase shift of $-\theta$, so it could be more experimentally feasible.

B. Inverse transformation with XPM process

Now we should transform the output single-photon qutrit back to a biphotonic qutrit. We apply the inverse transformation procedure shown in Fig. 5 and will show that it can be realized with a success probability as high as $\frac{1}{2}$.

At first, we apply a setup called entangler shown in dashed line to the transformed single-photon qutrit $|\psi'\rangle_S = \alpha'|H\rangle_0 + \beta'|H\rangle_1 + \gamma'|H\rangle_2$ with an ancilla single photon in the state $|\pm\rangle_a$, after a σ_x operation performed on the spatial modes 1 and 2, respectively. The entangler is to implement the transformation

$$|\psi'\rangle_S|+\rangle_a \to \alpha'|HH\rangle_{0,a} + \beta'|VV\rangle_{1,a} + \gamma'|VV\rangle_{2,a}, \tag{27}$$

where the polarization of the ancilla single photon will be the same as that of the single-photon qutrit. In the entangler, two qubus beams $|\alpha\rangle|\alpha\rangle$ are introduced and then coupled to the

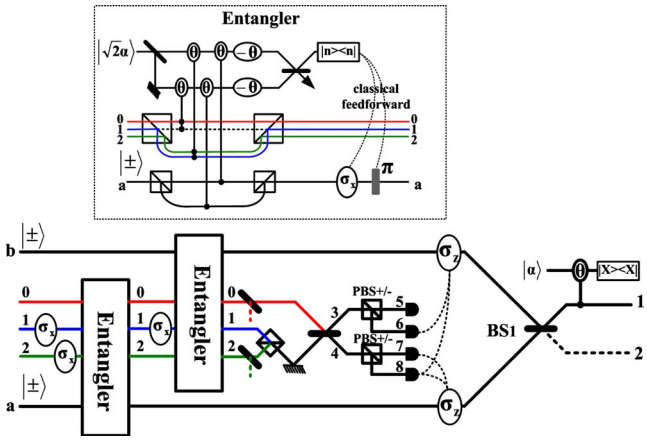

FIG. 5. (Color online) Schematic setup for the inverse transformation with XPM process. The part called entangler shown in dashed line entangles the single-photon qutrit and the ancilla single photon. Out of the entangler, the polarization of the ancilla photon will be the same as those of the single-photon qutrit. This inverse transformation can be implemented with a success probability 1/2.

corresponding photonic modes through the XPM processes. The XPM pattern in Fig. 5 is that the first beam being coupled to $|V\rangle$ modes on paths 1 and 2 and the $|H\rangle$ mode of the ancilla photon, while the second beam to $|H\rangle$ mode on path 0 and the $|V\rangle$ mode of the ancilla photon. Suppose the XPM phase shifts induced by the couplings are all θ. As the result, we will transform the total system to

$$\frac{1}{\sqrt{2}}(\alpha'|HH\rangle_{0,a}+\beta'|VV\rangle_{1,a} + \gamma'|VV\rangle_{2,a})|\alpha e^{i\theta}\rangle|\alpha e^{i\theta}\rangle+\frac{1}{\sqrt{2}}\alpha'|HV\rangle_{0,a}|\alpha\rangle|\alpha e^{i2\theta}\rangle + \frac{1}{\sqrt{2}}(\beta'|VH\rangle_{1,a}+\gamma'|VH\rangle_{2,a})|\alpha e^{i2\theta}\rangle|\alpha\rangle. \tag{28}$$

After that, a phase shifter of $-\theta$ is, respectively, applied to two qubus beams and then one more 50:50 BS implements the transformation $|\alpha_1\rangle|\alpha_2\rangle\rightarrow|\frac{\alpha_1-\alpha_2}{\sqrt{2}}\rangle|\frac{\alpha_1+\alpha_2}{\sqrt{2}}\rangle$ of the coherent-state components. The state of the total system will be therefore transformed to

$$\frac{1}{\sqrt{2}}(\alpha'|HH\rangle_{0,a}+\beta'|VV\rangle_{1,a}+\gamma'|VV\rangle_{2,a})|0\rangle|\sqrt{2}\alpha\rangle + \frac{1}{\sqrt{2}}\alpha'|HV\rangle_{0,a}|-i\sqrt{2}\alpha\sin\theta\rangle|\sqrt{2}\alpha\cos\theta\rangle+\frac{1}{\sqrt{2}}(\beta'|VH\rangle_{1,a} + \gamma'|VH\rangle_{2,a})|i\sqrt{2}\alpha\sin\theta\rangle|\sqrt{2}\alpha\cos\theta\rangle. \tag{29}$$

The first coherent-state component in Eq. (29) is either vacuum or a cat state (the superposition of $|\pm i\sqrt{2}\alpha\sin\theta\rangle$ in the second piece). The target output could be therefore obtained by the projection $|n\rangle\langle n|$ on the first qubus beam. If $n=0$, we will obtain

$$\alpha'|HH\rangle_{0,a}+\beta'|VV\rangle_{1,a}+\gamma'|VV\rangle_{2,a}, \tag{30}$$

with the polarization of ancilla photon the same to the single-photon qutrit. If $n\neq 0$, on the other hand, there will be the output

$$e^{-in\pi/2}\alpha'|HV\rangle_{0,a}+e^{in\pi/2}(\beta'|VV\rangle_{1,a}+\gamma'|VV\rangle_{2,a}), \tag{31}$$

which can be transformed to the form in Eq. (30) by a phase shift π following the classically feed-forwarded measurement result n and a σ_x operation on the ancilla photon.

Next, the second entangler will be applied to the above output and another ancilla single photon $|\pm\rangle_b$, after a σ_x operation is performed on spatial mode 1. In this entangler, the transmitted path for mode 1 is now active while the reflected port is only active in the first entangler. Similar to the first entangler, the second implements the transformation

$$(\alpha'|HH\rangle_{0,a}+\beta'|HV\rangle_{1,a}+\gamma'|VV\rangle_{2,a})|+\rangle_b\rightarrow\alpha'|HHH\rangle_{0,a,b} + \beta'|HVH\rangle_{1,a,b}+\gamma'|VVV\rangle_{2,a,b}. \tag{32}$$

Also, we need to erase the path information of the first photon. We first combine the modes 1 and 2 by a PBS and then make them interfere with the mode 0 through a 50:50 BS to achieve the following state:

$$\frac{\alpha'}{\sqrt{2}}(|H\rangle_3+|H\rangle_4)|HH\rangle_{a,b}+\frac{\beta'}{\sqrt{2}}(|H\rangle_3-|H\rangle_4)|VH\rangle_{a,b} + \frac{\gamma'}{\sqrt{2}}(|V\rangle_3-|V\rangle_4)|VV\rangle_{a,b}. \tag{33}$$

By two $\mathrm{PBS}_{\pm}$, the state

$$\frac{1}{2}(\alpha'|HH\rangle_{a,b}+\beta'|VH\rangle_{a,b}+\gamma'|VV\rangle_{a,b})|+\rangle_5+\frac{1}{2}(\alpha'|HH\rangle_{a,b} + \beta'|VH\rangle_{a,b}-\gamma'|VV\rangle_{a,b})|-\rangle_6+\frac{1}{2}(\alpha'|HH\rangle_{a,b}-\beta'|VH\rangle_{a,b} - \gamma'|VV\rangle_{a,b})|+\rangle_7+\frac{1}{2}(\alpha'|HH\rangle_{a,b}-\beta'|VH\rangle_{a,b} + \gamma'|VV\rangle_{a,b})|-\rangle_8 \tag{34}$$

will be then obtained. With four detectors on paths 5, 6, 7, and 8, as well as the classical feed forward, the state

$$\alpha'|HH\rangle_{a,b}+\beta'|VH\rangle_{a,b}+\gamma'|VV\rangle_{a,b} \tag{35}$$

will be finally realized. The above processes could be deterministic.

The final step is to merge the two photons into the same spatial mode, which could be simply realized by a BS and the following QND module. In this QND module, a qubus beam $|\alpha\rangle$ will be coupled to one of the output modes of BS_1. After that, the state in Eq. (35) plus the qubus beam will evolve to

$$\frac{1}{\sqrt{2}}\left(\alpha'|HH\rangle_{1,1}+\frac{1}{\sqrt{2}}\beta'|VH\rangle_{1,1}+\gamma'|VV\rangle_{1,1}\right)|\alpha e^{i2\theta}\rangle + \frac{1}{\sqrt{2}}\beta'(|VH\rangle_{1,2}+|VH\rangle_{2,1})|\alpha e^{i\theta}\rangle+\frac{1}{\sqrt{2}}\left(\alpha'|HH\rangle_{2,2} + \frac{1}{\sqrt{2}}\beta'|VH\rangle_{2,2}+\gamma'|VV\rangle_{2,2}\right)|\alpha\rangle. \quad (36)$$

Through the quadrature measurement $|X\rangle\langle X|$, the following state:

$$\alpha'|HH\rangle_{1,1}+\frac{1}{\sqrt{2}}\beta'|VH\rangle_{1,1}+\gamma'|VV\rangle_{1,1} \quad (37)$$

or

$$\alpha'|HH\rangle_{2,2}+\frac{1}{\sqrt{2}}\beta'|VH\rangle_{2,2}+\gamma'|VV\rangle_{2,2} \quad (38)$$

can be selected out and the output with only one photon at each output port, which picks up the phase shift θ in the XPM process, will be discarded. The different coefficients between the midterm and the other two terms in Eqs. (37) and (38) are caused by the Hong-Ou-Mandal (HOM) interference effect on BS_1. In order to balance the coefficients, we should use a 50:50 BS, respectively, on paths 0 and 2 (see Fig. 5). After that, we could achieve the biphotonic qutrit $\alpha'|0\rangle_3+\beta'|1\rangle_3+\gamma'|2\rangle_3$ with the success probability $\frac{1}{2}$ and then the total success probability for an arbitrary unitary operation on biphoton qutrits will be $\frac{1}{6}\times\frac{1}{2}=\frac{1}{12}$.

IV. DISCUSSION

We have presented two schemes for unitary operations on biphoton qutrits, which are realized through bi-directional mapping between polarization and spatially encoded photonic qutrits. Through the bi-directional mapping, any unitary operation U(3) on biphotonic qutrits can be reduced to that on single-photon qutrits. The linear optical scheme succeeds with a small probability 1.17×10^{-4}, but it can be increased to 1/12 with weak cross-Kerr nonlinearity. The probabilistic nature of the schemes is due to the two indistinguishable photons in the same spatial-temporal modes. For example, at the last merging step in Fig. 5, the probability to get the proper output state will be lowered by 1/2 because of the HOM interference.

Finally, we look at the feasibility of the schemes. The first scheme applies common experimental tools such as linear optical circuits, coincidence measurements, and detection with APDs. The difficulty in the implementation is the accuracy for the numerous interferences between the photonic modes. The additional requirement in the second scheme is the good performance of weak cross-Kerr nonlinearity. The error in each XPM process can be effectively eliminated under the condition $\alpha\theta\gg1$ [16], which means that the small XPM phase θ can be compensated by the large amplitude $|\alpha|$ of the qubus or communication beams. The other advantage of the scheme based on weak nonlinearity is the fewer ancilla photons—the ancilla photons are only required in the inverse transformation. This could make the experimental implementation more simplified.

ACKNOWLEDGMENTS

Q.L. thanks Dr. Jian Li and Ru-Bing Yang for helpful discussions.

[1] N. K. Langford, R. B. Dalton, M. D. Harvey, J. L. OBrien, G. J. Pryde, A. Gilchrist, S. D. Bartlett, and A. G. White, Phys. Rev. Lett. **93**, 053601 (2004); R. W. Spekkens and T. Rudolph, Phys. Rev. A **65**, 012310 (2001); G. Molina-Terriza, A. Vaziri, J. Rehacek, Z. Hradil, and A. Zeilinger, Phys. Rev. Lett. **92**, 167903 (2004); S. Gröblacher *et al.*, New J. Phys. **8**, 75 (2006); D. Bruß and C. Macchiavello, Phys. Rev. Lett. **88**, 127901 (2002); N. J. Cerf, M. Bourennane, A. Karlsson, and N. Gisin, *ibid.* **88**, 127902 (2002); T. Durt, N. J. Cerf, N. Gisin, and M. Zukowski, Phys. Rev. A **67**, 012311 (2003).

[2] T. C. Ralph, K. Resch, and A. Gilchrist, Phys. Rev. A **75**, 022313 (2007); B. P. Lanyon *et al.*, Nat. Phys. **5**, 134 (2009).

[3] A. Mair *et al.*, Nature (London) **412**, 313 (2001); A. Vaziri, G. Weihs, and A. Zeilinger, Phys. Rev. Lett. **89**, 240401 (2002).

[4] L. Neves, S. Padua, and C. Saavedra, Phys. Rev. A **69**, 042305 (2004); L. Neves, G. Lima, J. G. Aguirre Gomez, C. H. Monken, C. Saavedra, and S. Padua, Phys. Rev. Lett. **94**, 100501 (2005); M. N. O'Sullivan-Hale, I. A. Khan, R. W. Boyd, and J. C. Howell, *ibid.* **94**, 220501 (2005).

[5] R. T. Thew, A. Acin, H. Zbinden, and N. Gisin, Phys. Rev. Lett. **93**, 010503 (2004); H. de Riedmatten, I. Marcikic, V. Scarani, W. Tittel, H. Zbinden, and N. Gisin, Phys. Rev. A **69**, 050304(R) (2004).

[6] J. C. Howell, A. Lamas-Linares, and D. Bouwmeester, Phys. Rev. Lett. **88**, 030401 (2002); Y. I. Bogdanov, M. V. Chekhova, S. P. Kulik, G. A. Maslennikov, A. A. Zhukov, C. H. Oh, and M. K. Tey, *ibid.* **93**, 230503 (2004); E. V. Moreva, G. A. Maslennikov, S. S. Straupe, and S. P. Kulik, *ibid.* **97**, 023602 (2006); G. Vallone, E. Pomarico, F. De Martini, P. Mataloni, and M. Barbieri, Phys. Rev. A **76**, 012319 (2007); Y. Li, K. Zhang, and K. Peng, *ibid.* **77**, 015802 (2008).

[7] H. Mikami and T. Kobayashi, Phys. Rev. A **75**, 022325 (2007).

[8] B. P. Lanyon, T. J. Weinhold, N. K. Langford, J. L. O'Brien, K. J. Resch, A. Gilchrist, and A. G. White, Phys. Rev. Lett. **100**, 060504 (2008).

[9] If we adopt the notation $|0\rangle_{3'}\equiv|HH\rangle$, $|1\rangle_{3'}\equiv\frac{1}{\sqrt{2}}(|HV\rangle+|VH\rangle)$, $|2\rangle_{3'}\equiv|VV\rangle$ in [8], there will be no difference from the results obtained in the present paper, since any input in this basis can be represented as $|\psi\rangle_{in}+\mathcal{P}|\psi\rangle_{in}$, where $\mathcal{P}$ refers to the permutation of two indistinguishable photons and $|\psi\rangle_{in}=\frac{\alpha}{2}|0\rangle_3+\frac{\beta}{\sqrt{2}}|1\rangle_3+\frac{\gamma}{2}|2\rangle_3$ is the qutrit defined in the logic basis of Eq. (1).

[10] Y. I. Bogdanov, M. V. Chekhova, L. A. Krivitsky, S. P. Kulik, A. N. Penin, A. A. Zhukov, L. C. Kwek, C. H. Oh, and M. K.

Tey, Phys. Rev. A **70**, 042303 (2004).
[11] M. Reck, A. Zeilinger, H. J. Bernstein, and P. Bertani, Phys. Rev. Lett. **73**, 58 (1994).
[12] C. K. Hong, Z. Y. Ou, and L. Mandel, Phys. Rev. Lett. **59**, 2044 (1987).
[13] M. A. Nielsen and I. L. Chuang, *Quantum Computation and Quantum Information* (Cambridge University Press, Cambridge, England, 2000).
[14] S. D. Barrett, P. Kok, K. Nemoto, R. G. Beausoleil, W. J. Munro, and T. P. Spiller, Phys. Rev. A **71**, 060302(R) (2005).
[15] K. Nemoto and W. J. Munro, Phys. Rev. Lett. **93**, 250502 (2004).
[16] W. J. Munro, K. Nemoto, and T. P. Spiller, New. J. Phys. **7**, 137 (2005); T. P. Spiller, K. Nemoto, S. L. Braunstein, W. J. Munro, P. van Loock, and G. J. Milburn, *ibid.* **8**, 30 (2006).
[17] Q. Lin and J. Li, Phys. Rev. A **79**, 022301 (2009).
[18] B. He, Y.-H. Ren, and J. A. Bergou, Phys. Rev. A **79**, 052323 (2009).
[19] P. Kok, Phys. Rev. A **77**, 013808 (2008).
[20] S. E. Harris and L. V. Hau, Phys. Rev. Lett. **82**, 4611 (1999); W. J. Munro, K. Nemoto, R. G. Beausoleil, and T. P. Spiller, Phys. Rev. A **71**, 033819 (2005); D. A. Braje, V. Balic, G. Y. Yin, and S. E. Harris, *ibid.* **68**, 041801(R) (2003).
[21] T. J. Kippenberg, S. M. Spillane, and K. J. Vahala, Phys. Rev. Lett. **93**, 083904 (2004).
[22] X. Li, P. L. Voss, J. E. Sharping, and P. Kumar, Phys. Rev. Lett. **94**, 053601 (2005).
[23] P. Grangier, J. A. Levenson, and J.-P. Poizat, Nature (London) **396**, 537 (1998); Q. A. Turchette, C. J. Hood, W. Lange, H. Mabuchi, and H. J. Kimble, Phys. Rev. Lett. **75**, 4710 (1995).